A Two-Stage GA-Based sEMG Feature Selection Method for User-Independent Continuous Estimation of Elbow Angles

He Li, *Graduate Student Member, IEEE*, Shuxiang Guo, *Fellow, IEEE*, Dongdong Bu, *Graduate Student Member, IEEE*, and Hanze Wang, *Student Member, IEEE*

***Abstract*— Surface electromyography (sEMG) has great application potential in upper extremity rehabilitation exoskeleton. The accurate identification of elbow motion angle is crucial for the sEMG-controlled upper limb exoskeleton rehabilitation system. However, the existing high intersubject variability in sEMG limits the generality of the model built through learning algorithms among different subjects. Aiming at the above problem, a feature selection method based on a two-stage genetic algorithm (GA) is proposed for the accurate user-independent estimation of continuous movements. And the information theory-based minimum redundancy maximum relevance criterion serves as the fitness function to evaluate the goodness of subsets. The effectiveness of the proposed method is verified by estimating the motion angle of the elbow joint using the collected sEMG data of six participants. The prediction performance is compared with that before the two-stage GA-based feature selection (TS-GAFS), and different metrics and statistical analyses are adopted to evaluate the results. The estimation angle error calculated after TS-GAFS is controlled within 10°, which shows the feasibility of the proposed method for the accurate user-independent estimation of continuous joint movements.**

***Index Terms*— Continuous estimation, feature selection, information theory, intersubject variability, surface electromyography (sEMG), two-stage genetic algorithm (GA).**

I. Introduction

WITH the continuous improvement in medical science, the average life expectancy gradually increases, increasing the size of the older population, which in turn is accompanied by a rise in the numbers of geriatric diseases and complications. One such geriatric disease is stroke [1], causing motor impairments and disability in more than half of the patients. And upper limb hemiparesis is one of the primary impairments following the stroke, which leads to stiffness and weakened muscular strength on the hemiplegic side, then consequently reduced range of motion (ROM), and finally negatively affecting the activities of daily living (ADL) [2]. Upper extremity hemiparesis brings not only pain to patients, but also a heavy burden on families. Based on the remolding theory of brain injury, nerve stimulation through rehabilitation training can increase automatic nerve repair [3]. Therefore, timely rehabilitation training is necessary.

Traditional rehabilitation therapy has a positive impact on the recovery of stroke hemiplegia, but this one-on-one, repeatable, and labor-intensive rehabilitation therapy leads to a serious shortage of rehabilitation therapists; patients' families need to bear heavy economic pressure, so it cannot guarantee the effectiveness of long-term rehabilitation therapy. But with the development of robotics, robots can undertake highly repetitive and high-precision work, and rehabilitation robots combining robotics and rehabilitation medicine can well-solve the problems faced by the traditional rehabilitation therapy [4], [5]. For hemiplegic patients, the upper limb exoskeleton device has been successfully combined with some rehabilitation training strategies, such as the bilateral rehabilitation strategy that uses the contralateral side to drive the affected side to perform synchronous movements [6], [7], [8]. During bilateral training, surface electromyography (sEMG) as a noninvasive approach can be used to extract the motion information of the intact side. Due to the inherent intuitiveness and effectiveness of sEMG [9], the exoskeleton device worn by the affected side can be controlled by sEMG of the intact side.

The noninvasive and easily acquired sEMG method makes it possible to provide control signals to the exoskeleton [10] even if the limb does not move, as long as there are sEMG signals, which allows elderly people with weak muscle strength to exercise by wearing exoskeletons. Hence, taking sEMG as the control signal is almost tailor-made for upper limb rehabilitation exoskeletons. However, there still exist some shortcomings of the using of sEMG, in which intersubject variability is one typical representative. Since sEMG signals have a user-specific nature, causing the amplitude and frequencies to be highly variable among different subjects [11], that is, high

Manuscript received 7 November 2022; revised 23 March 2023; accepted 2 May 2023. Date of publication 15 May 2023; date of current version 1 June 2023. This work was supported in part by the National Natural Science Foundation of China under Grant 61703305, in part by the National High-Tech Research and Development Program (863 Program) of China under Grant 2015AA043202, and in part by the Special Project of Science (SPS) KAKENHI under Grant 15K2120. The Associate Editor coordinating the review process was Dr. David Ayllon. *(Corresponding author: Shuxiang Guo.)*

This work involved human subjects or animals in its research. Approval of all ethical and experimental procedures and protocols was granted by the Institutional Review Board (IRB) in the Faculty of Engineering Kagawa University under Ref. No. 01-011 from February 2020, and performed in line with the Declaration of Helsinki.

He Li, Dongdong Bu, and Hanze Wang are with the School of Life Science and the Key Laboratory of Convergence Biomedical Engineering System and Healthcare Technology, The Ministry of Industry and Information Technology, Beijing Institute of Technology, Beijing 100081, China (e-mail: lihe@bit.edu.cn).

Shuxiang Guo is with the School of Life Science and the Key Laboratory of Convergence Biomedical Engineering System and Healthcare Technology, The Ministry of Industry and Information Technology, Beijing Institute of Technology, Beijing 100081, China, and also with the Department of Electronic and Electrical Engineering, Southern University of Science and Technology, Shenzhen, Guangdong 518055, China (e-mail: guoshuxiang@bit.edu.cn).

Digital Object Identifier 10.1109/TIM.2023.3276522

intersubject variability is inevitable. Li et al. [12] evaluated the influence of intersubject variability for elbow continuous motion through a shallow neural network. To reduce the error from individual differences, Yang et al. [13] built models for each user. However, there exists a too large workload in this method. Once a new user is added, enough data from this user need to be collected to train a new model for it. To extract the most suitable features from the accelerometer data, Saputri et al. [14] proposed a feature selection method by analyzing features based on subject and activity behavior. However, it aimed to use acceleration data for activity recognition without involving sEMG signals at all. Xiong et al. [15] proposed a user-independent gesture recognition approach based on sEMG decomposition. However, it is only aimed at the classification of five discrete gestures and does not involve the recognition of joint continuous motion. In summary, to the best of authors' knowledge, no one has proposed a feature selection method considering the intersubject variability on sEMG for subject-independent estimation of continuous movements.

In this article, a two-stage genetic algorithm (GA)-based feature selection (TS-GAFS) method is proposed. The TS-GAFS method is the extension of the GA algorithm, which further considers the demand for subject-independent prediction of continuous motion. Through feature selection, relatively stable features among different subjects can be selected to improve the prediction performance. In detail, time-domain (TD) features of sEMG are selected according to the proposed TS-GAFS method. The selected subject-independent feature subset is the input of the neural network to predict continuous movements of elbow joints. Further, quantitative analysis realized through evaluation criteria and Bland–Altman (B&A) plot is performed. It can be demonstrated through the experiments that the model established after feature selection has a better estimation effect compared with that before feature selection, which shows the effectiveness of our proposed TS-GAFS method for user-independent continuous estimation of joint movements. The main contributions are as follows.

1) Considering the intersubject variability of sEMG, the TS-GAFS method is proposed to extract the common feature subset among different subjects.
2) Based on the proposed method, the subject-independent estimation of continuous movements is realized, which verifies the validity of the method.

The rest of this article is organized as follows. The experimental scheme is described in Section II. The proposed method for subject-independent continuous estimation of elbow angle is elaborated in Section III. The results and discussion of this study are reported in Section IV. Finally, the conclusion and future work are drawn in Section V.

II. Experimental Scheme

A. Participants and Experimental Paradigm

In this article, six healthy subjects (four males and two females, denoted as subjects A–F, respectively) are chosen. All the participating subjects have no musculoskeletal disorders.

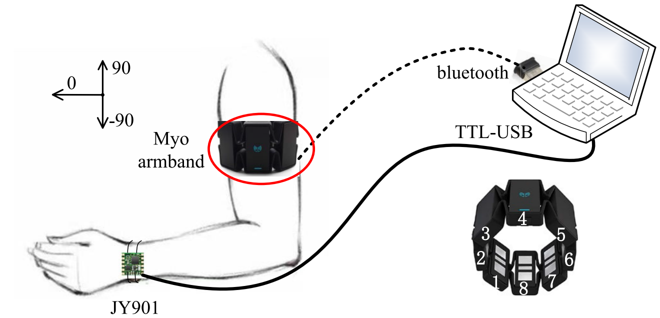

Fig. 1. Schematic of sEMG acquisition.

Before the experiment, all participating subjects are informed of the experimental procedure and given informed consents.

Before the signal acquisition, subjects are told that their upper and forearms should be relaxed to avoid muscle tension, which could introduce shifts. To ensure that the upper limb moves with only one degree of freedom (the vertical plane), the subject's wrist should be kept along with the forearm. The forearm starts in the natural sagging position, moves around the elbow joint, and then returns to the natural sagging position. Continue the above motion for one minute. Each subject repeats the experimental procedure five times with two-minute rest between two adjacent experiments to avoid muscle fatigue. Since the sampling frequency of Myo armband is 200 Hz, the number of sampling points is 12 000 for each subject in each time of experiments.

B. Experimental Setup

Each subject's sEMG data is acquired using Myo armband (Thalmic Labs, Canada), which is a commercially available device [16]. The acquisition schematics of sEMG are shown in Fig. 1. During the experiment, Myo is worn at the same location of each user's upper arm as the fourth-channel sensor of Myo armband corresponds to the biceps brachii. The sEMG data are sampled at 200 Hz and then directly streamed to the workspace of MATLAB (2020b, MathWorks, USA) using a custom-written script through Bluetooth communication. Besides Myo armband, an angle sensor (JY901, WIT motion, sampling frequency: 20 Hz) is tied on the forearm to record the actual angle that is considered as the target value.

C. Channel Selection of Myo Armband

The number of channels affects the prediction performance of sEMG data acquired by Myo armband. Channel selection for sEMG signal is a very important task, which can reduce information redundancy and then improve the speed and accuracy of later modeling. According to [17], the suggested number of channels is 3 that is the channel number adopted in this article, and the three channels are the fourth channel, the seventh channel, and the first channel, respectively. The fourth channel and the seventh channel are selected according to the position of biceps and triceps brachii, that is, the fourth channel and the seventh channel collect the sEMG signals corresponding to the two muscles, respectively. The first channel is selected according to the mutual information

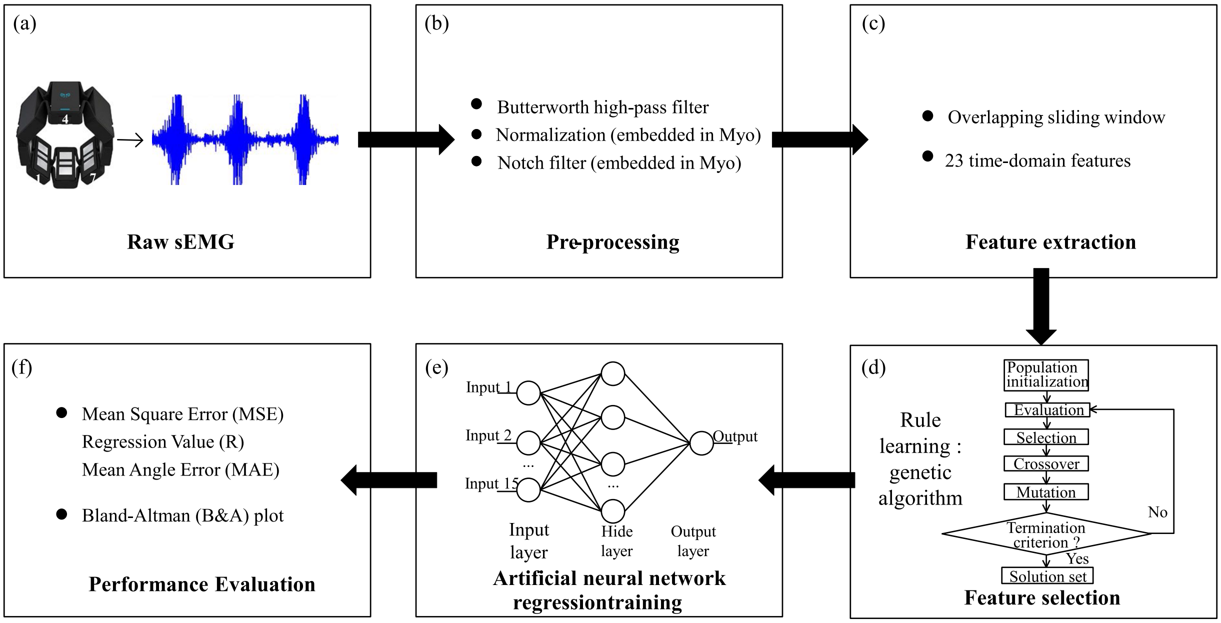

Fig. 2. Adopted method for subject-independent continuous estimation of elbow angles on sEMG data using neural network with GAFS.

TABLE I

REDUNDANCY CALCULATION RESULTS BETWEEN THE FOURTH CHANNEL (SEVENTH CHANNEL) AND OTHER CHANNELS (FIRST CHANNEL, SECOND CHANNEL, THIRD CHANNEL, FIFTH CHANNEL, SIXTH CHANNEL, AND EIGHTH CHANNEL)

	4th channel	7th channel	Average
1st channel	0.1664	0.0986	0.1325
2nd channel	0.4892	0.0804	0.2848
3rd channel	0.8303	0.1179	0.4741
5th channel	0.7478	0.1933	0.4706
6th channel	0.2974	0.4165	0.3570
8th channel	0.0340	0.2763	0.1552

concept (maximum synergy and minimum redundancy), that is, the average redundancy degree of the first channel and the jth channel ($j = 4, 7$) is the smallest compared to other channels (second, third, fifth, sixth, and eighth channels). Take the sEMG data of subject A as an example (the data of other subjects have the same conclusion), and Table I shows the calculation results of redundancy. As can be seen from Table I, the first channel has the lowest redundancy degree with the fourth channel and the seventh channel.

III. METHODS

The overall schematic of the proposed method for continuous estimation of elbow angle is illustrated in Fig. 2. The first step (step B) is the preprocessing of the raw sEMG acquired according to the above experimental scheme. The second step (step C) is the feature extraction based on time-domain features. The third step (step D) is the feature selection method for subject-independent continuous angle estimation using GA. The learning process for angle regression is done in the fourth step (step E) using a neural network, based on selected features. Finally, evaluation criteria and a statistical approach are used to evaluate the results.

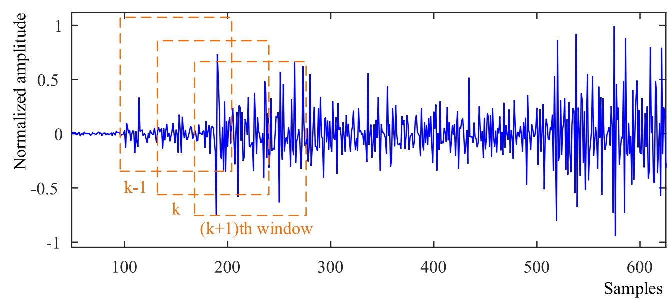

Fig. 3. Schematic of the sliding window approach illustrated for the case of sEMG.

A. Preprocessing of sEMG Signal

Raw sEMG is a very weak and vulnerable biological signal. To obtain high-quality signals, the data preprocessing step is indispensable. The sEMG has been normalized to $[-1\ 1]$ and filtered at 50 Hz through the software development kit of Myo. Hence, a high-pass filter (fourth-order Butterworth) at 20 Hz is then applied to the signal to remove direct current offsets and the low-frequency noises.

B. Feature Extraction

Because sEMG is highly nonstationary, to ensure the continuity of the features, the combination of the time window and incremental window is used for feature extraction, and the schematic of the sliding window approach is shown in Fig. 3. Considering the real-time requirements of human–robot interfaces (HRIs), the length of time window cannot exceed 300 ms [18]. In this article, the window length is 250 ms (the corresponding sampling point number is 50) with an increment of 100 ms (the corresponding sampling point number is 20). Therefore, the number of sliding windows for each subject in each time of experiments is 598, as calculated by the following equation:

$$N_{\text{win}} = \frac{1}{L_{\text{add}}}(N_{\text{sam}} - L_{\text{win}} + L_{\text{add}}) \tag{1}$$

TABLE II
NOTATION OF THE 23 TD FEATURES

F1	F2	F3	F4	F5	F6	F7	F8	F9
IAV	MAV	RMS	SSC	ZC	ARC	KURT	LogD	MarginFac
F10	F11	F12	F13	F14	F15	F16	F17	F18
MAX	MEAN	MIN	NZM	PeakFac	PK	PulsFac	SKEW	SSI
F19	F20	F21	F22	F23				
STD	VAR	WA	WavFac	WL				

where N_{win}, N_{sam}, L_{win}, and L_{add} represents the number of sliding windows for each subject in each time of experiments, the number of sampling points for each subject in each time of experiments, the window length, and the window increment, respectively.

Based on the segmented sliding window, different features are extracted from each window to build a feature vector [19], which is used to estimate the angle of joint movements. Thus far, TD features, frequency-domain (FD) features, and time–frequency domain (TFD) features have been widely adopted for sEMG signal processing [19], [20]. Considering that TD features are closely associated with sEMG amplitude, which directly reflects the angle information. Therefore, 23 TD features are extracted in this article, and the full name of these features is recorded in the Appendix, corresponding to F1–F23, respectively, as shown in Table II.

C. Proposed TS-GAFS Method

The main purpose of feature selection is to select relevant features from all features or remove irrelevant features and redundant features without losing important information. Feature selection has a high impact on the effect of angle estimation; a subset of the available features can be selected for the application of learning algorithms [20], [21]. After feature selection, the curse of dimensionality can be avoided, and the estimation accuracy can be increased. Furthermore, in most applications, the use of feature selection can reduce the cost of the system.

According to the combination of subset evaluation criteria and the subsequent learning algorithm, feature selection can be divided into three categories: embedded method, filter method, and wrapper method. In the embedded method, the feature selection algorithm itself is embedded as part of the learning algorithm. The evaluation criteria of the filter method are obtained from the inherent properties of the dataset itself, independent of specific learning algorithms, so it has a good universality to different learning algorithms. The wrapper method uses the performance of the learning algorithm to evaluate the features themselves. Therefore, embedded and wrapper methods lack generalization ability due to their reliance on a specific learning algorithm. When modifying the estimator embedded in the wrapper and embedding methods, the selected subset of features may not be suitable, and thus, the feature selection process needs to be repeated. Based on the above, considering the generality of feature subsets, the filter method is adopted in this article.

The GAFS method is adopted in this article, and the information theory-based minimum redundancy maximum relevance (mRMR) criterion [22] is used as the fitness function to evaluate the feature subsets. GA evaluates features by selecting feasible individuals from the population to find the maximum fitness of the population; then, the genetic information is used to generate a new optimal population of solution. GA can effectively reduce the possibility of inevitably falling into local optimum in practical optimization problems [23]. The principle of GA that consists of two basic operations (crossover and mutation) is to use GA to find an optimal binary code. And each bit in the code corresponds to a feature, if the ith bit is "1," it means that the corresponding feature is selected [as shown in (2)], and the feature will appear in the estimator; if the ith bit is "0," it means that the corresponding feature is not selected [as shown in (2)], and the feature will not appear in the estimator

$$\text{gene index}\begin{cases}1, & \text{if the feature is selected}\\ 0, & \text{otherwise.}\end{cases} \tag{2}$$

Based on the aim that finding the feature subset that is most appropriate for angle estimation among different subjects, the TS-GAFS method is proposed in this article, in which the first stage is based on each subject, and the second stage is based on all subjects. The following describes the two stages, respectively.

In the first stage of the TS-GAFS method, the features of each subject are analyzed, respectively, and the features that have a high impact on the motion angle for each subject can be determined. The specific steps are as follows: for each subject, use the GAFS algorithm to select ten features, run the algorithm five times, and take the union of the results of the five runs as each subject's feature subset, as recorded in Table III. Perform the above steps for each subject to obtain the feature subset of each subject, and finally take the intersection of these feature subsets of all subjects to determine the final feature subset of the first stage, as recorded in Table IV. The feature subset selected in this stage serves as the input for the second stage that follows.

In the second stage of the TS-GAFS method, the features of all subjects are analyzed comprehensively. The features that are used as the input in this stage are the feature subsets determined in the first stage. The specific steps are as follows: run the GAFS algorithm five times using the samples of all subjects, and take the intersection of the results of the five runs as the final feature subset of all subjects, as recorded in Table V. Through the above process, the most common

TABLE III
FEATURE SELECTION RESULTS FOR EACH USER IN THE FIRST STAGE

User	Times	Features												
		1	2	3	4	5	6	7	8	9	10	11	12	13
User A	1st	F1	F2	F7	F9	F10	F16	F18	F19	F20	F23			
	2nd	F2	F3	F9	F10	F14	F16	F18	F19	F22	F23			
	3rd	F1	F2	F3	F7	F9	F10	F16	F18	F20	F23			
	4th	F2	F3	F9	F10	F14	F16	F18	F19	F22	F23			
	5th	F1	F2	F9	F10	F14	F16	F18	F19	F20	F22			
	Union	F1	F2	F3	F7	F9	F10	F14	F16	F18	F19	F20	F22	F23
User B	1st	F1	F2	F3	F7	F9	F10	F16	F18	F19	F20			
	2nd	F2	F3	F7	F8	F9	F15	F16	F18	F19	F20			
	3rd	F1	F2	F3	F7	F9	F10	F16	F18	F19	F20			
	4th	F1	F2	F3	F7	F9	F10	F16	F18	F19	F20			
	5th	F1	F2	F3	F7	F9	F10	F16	F18	F19	F20			
	Union	F1	F2	F3	F7	F8	F9	F10	F15	F16	F18	F19	F20	
User C	1st	F1	F2	F7	F10	F14	F16	F18	F19	F20	F22			
	2nd	F2	F7	F9	F10	F16	F18	F19	20	F22	F23			
	3rd	F1	F2	F7	F14	F15	F16	F18	F19	F20	F22			
	4th	F1	F7	F9	F10	F16	F18	F19	F20	F22	F23			
	5th	F2	F7	F9	F10	F16	F18	F19	F20	F22	F23			
	Union	F1	F2	F7	F9	F10	F14	F15	F16	F18	F19	F20	F22	F23
User D	1st	F2	F7	8	F9	F10	F16	F18	F19	F20	F23			
	2nd	F1	F2	F7	F8	F9	F10	F16	F18	F19	F20			
	3rd	F1	F2	F7	F9	F10	F16	F18	F19	F20	F23			
	4th	F1	F2	F7	F8	F9	F10	F16	F18	F19	F20			
	5th	F1	F2	F3	F7	F9	F10	F16	F18	F20	F23			
	Union	F1	F2	F3	F7	F8	F9	F10	F16	F18	F19	F20	F23	
User E	1st	F1	F2	F7	F9	F10	F16	F18	F19	F20	F22			
	2nd	F1	F2	F7	F9	F10	F16	F18	F19	F20	F22			
	3rd	F1	F2	F7	F9	F16	F18	F19	F20	F22	F23			
	4th	F2	F7	8	F9	F10	F16	F18	F19	F20	F22			
	5th	F1	F2	F7	F9	F10	F16	F19	F20	F22	F23			
	Union	F1	F2	F7	F8	F9	F10	F16	F18	F19	F20	F22	F23	

TABLE IV
FEATURE SELECTION RESULTS FOR ALL USERS IN THE FIRST STAGE

Users	Features												
	1	2	3	4	5	6	7	8	9	10	11	12	13
User A	F1	F2	F3	F7	F9	F10	F14	F16	F18	F19	F20	F22	F23
User B	F1	F2	F3	F7	F8	F9	F10	F15	F16	F18	F19	F20	
User C	F1	F2	F7	F9	F10	F14	F15	F16	F18	F19	F20	F22	F23
User D	F1	F2	F3	F7	F8	F9	F10	F16	F18	F19	F20	F23	
User E	F1	F2	F7	F8	F9	F10	F16	F18	F19	F20	F22	F23	
Intersection	F1	F2	F7	F9	F10	F16	F18	F19	F20				

features for all subjects can be determined. As shown in Table V, five features (F1, F2, F16, F19, and F20) are selected as the final feature subset. Then, the feature vector can be constructed based on the selected Myo channel and TD features. Specifically, the number of the selected Myo channels is 3 (the first channel, the fourth channel, and the seventh channel), and the number of the selected features is 5 (F1, F2, F16, F19, and F20). Based on the above, a 15-D feature vector is constructed.

D. Modeling for Continuous Angle Estimation

After getting the most common feature subset for all subjects, continuous motion estimation is the next step. In this article, the back propagation neural network (BPNN) is used for regression and prediction. The feature subset determined from the proposed TS-GAFS method is the input of the input layer of the BPNN. The number of input-layer nodes is consistent with the dimension of the feature vector, that is, the number of input-layer nodes is 15. According to the Kolmogorov superposition theorem, the number of hidden-layer nodes should be $2n + 2$, where n is the number of input-layer nodes. Therefore, the number of hidden-layer units is set at 32. The number of neurons in each layer of the network and the activation functions are recorded in Table VI. Through the neural network, the estimated angles of elbow movements can be calculated. Further to ensure that sEMG can be used as the

TABLE V
FEATURE SELECTION RESULTS FOR ALL USERS IN THE SECOND STAGE

Times	Features				
	1	2	3	4	5
1st	F1	F2	F16	F19	F20
2nd	F1	F2	F16	F19	F20
3rd	F1	F2	F16	F19	F20
4th	F1	F2	F16	F19	F20
5th	F1	F2	F16	F19	F20
Intersection	F1	F2	F16	F19	F20

TABLE VI
PARAMETERS OF NEURAL NETWORK

Number of neurons			Activation function		Performance function	Training function
Input layer	Hidden layer	Output layer	Hidden layer	Output layer		
15	32	1	tansig	purelin	MSE	trainlm

control signal of HRIs, an eight-point sliding window is used for filtering.

E. Evaluation Criteria

In this article, quantitative evaluation indicators of regression value (R), mean square error (MSE), and mean absolute error (MAE) are used to evaluate the estimation performance. In addition, B&A statistical method is also adopted for analysis. MSE and R are the evaluation indicators in the modeling process. MSE is the mean of the sum of squares of the differences between the predicted value and the target value, as shown in (3). R measures the correlation between outputs and targets, and the larger the R, the closer the relationship between the predicted values and the target values. MAE is the average error between output angles and target angles, as shown in (4). B&A plots are used to compare the consistency between two measurement data (the estimated angles and the target angles recorded by JY901)

$$\mathrm{MSE} = \frac{1}{N}\sum_{i=1}^{N}\left(\hat{y}_i - y_i\right)^2 \tag{3}$$

$$\mathrm{MAE} = \frac{1}{N}\sum_{i=1}^{N}\left|\hat{y}_i - y_i\right| \tag{4}$$

where y_i represents the actual value at the ith sampling point and $\hat{y}_i$ is the estimated value at the ith sampling point, and N is the total number of sampling points.

IV. RESULTS AND DISCUSSION

In this section, the models obtained through BPNN are showed and discussed. To verify the effectiveness of the proposed method in the application of continuous angle estimation of elbow joints, the comparison of modeling and prediction effect before and after TS-GAFS is provided.

A. Regression Effect Before and After TS-GAFS

In this study, a leave one-subject-out test method is adopted. That is, subject A–subject F serve as the test set in turn. Although the specific values of the evaluation indicators will change with different test sets, the conclusion is the same in each case. Therefore, normal one of the cases is taken as an example for analysis; this kind of case is that subject F is used as the additional test and subjects A–E are used for modeling. The total sEMG segments are 14 950, as calculated by (5). Samples are randomly divided into training, validation, and test sets; the ratio is 70%:15%:15%. Therefore, the sEMG segments of training set are 10 464, and the sEMG segments of both test and validation sets are 2243. The regression values of training, validation, and test sets are recorded during the training process (Table VII). The regression plots before and after TS-GAFS are shown in Fig. 4, respectively. As can be seen from Table VII, R and MSE after TS-GAFS are all better than that before TS-GAFS whether for training, validation, test data, or all data

$$N_{\mathrm{sEMG}} = N_{\mathrm{sub}} \times N_{\exp} \times N_{\mathrm{win}} \tag{5}$$

where N_{sEMG}, N_{sub}, $N_{\exp}$, and N_{win} represents the number of total sEMG segments, the number of subjects, the number of experiments for each subject, and the number of sliding windows for each subject in each time of experiments, respectively, in turn.

B. Estimation Comparison Before and After TS-GAFS

In this section, the comparison of the estimation result of subject F which is the additional test will be illustrated, as recorded in Table VIII. The value of MSE dropped from 421.1892 before TS-GAFS to 272.3429 after TS-GAFS, R increased from 0.8971 before TS-GAFS to 0.9478 after TS-GAFS, and MAE dropped from 14.4329 before TS-GAFS to 8.9542 after TS-GAFS. Therefore, it can be concluded from Table VIII that the estimation results of subject F after TS-GAFS are better than that before TS-GAFS.

Fig. 5 records the motion curve of target angles and estimated angles. Fig. 5(a) shows the obvious filtering effect, which verifies the applicability of the filtering algorithm, and only the filtered results can be further used in HRIs. Fig. 5(b) plots the estimated angle before and after TS-GAFS; it can

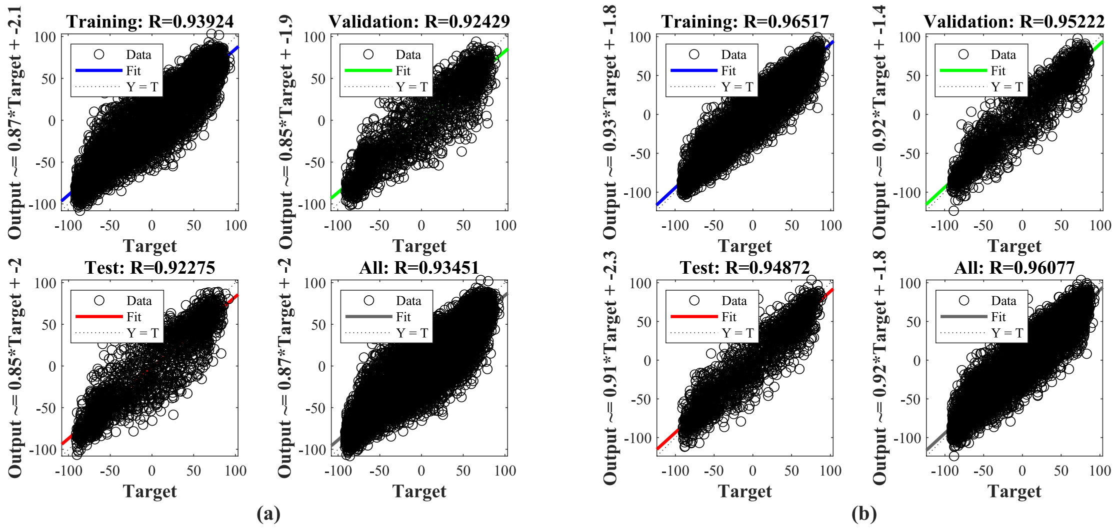

Fig. 4. Regression of BPNN model during training: (a) before TS-GAFS method and (b) after TS-GAFS method.

TABLE VII
MODELING PERFORMANCE OF BPNN

	Training		Validation		Test		R
	R	MSE	R	MSE	R	MSE	
Before	0.9392	358.4358	0.9243	453.0930	0.9228	451.0251	0.9345
After	0.9652	210.3576	0.9522	284.9693	0.9487	302.6596	0.9608

TABLE VIII
ESTIMATION COMPARISON OF THE ADDITIONAL TEST BEFORE AND AFTER TS-GAFS

	MSE	R	MAE
Before TS-GAFS	421.1892	0.8971	14.4329
After TS-GAFS	272.3429	0.9478	8.9542

be seen intuitively that the estimated angles after TS-GAFS are closer to the target angles. The B&A plots of estimated and actual angles are shown in Fig. 6, which shows that the data distribution after TS-GAFS is more centralized than that before TS-GAFS. And the "Mean" value after TS-GAFS (value = 1.3) is far less than that before TS-GAFS (value = 5.1), indicating that the prediction result of the model after TS-GAFS is closer to the actual angle value.

Among different subjects, sEMG signals vary greatly in both amplitude and spectrum, so there exists high intersubject variability. Furthermore, when the number of features is large, some features may be against each other. From the result, it can be found that the effect of regression and estimation results using the entire 23 features is not as good as that using the selected subset of features for understanding sEMG signals generated by different subjects. Therefore, it can be concluded that the proposed TS-GAFS method can help to select the most common feature subset for better subject-independent angle estimation. Moreover, the reduction in the number of features can reduce the computational burden and the performance of real-time control of the exoskeleton device can be improved.

According to Fig. 5 and Table VIII, the estimation performance of the proposed TS-GAFS method is effective. The estimation performance under the leave one-subject-out test is shown in Table IX, in which the regression values of different

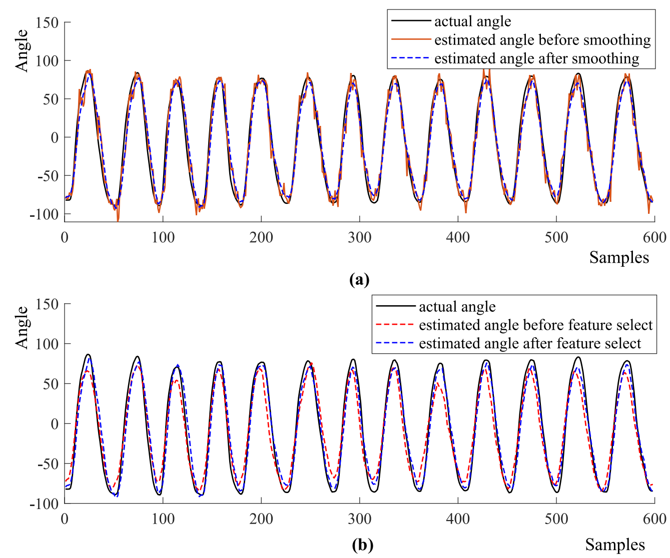

Fig. 5. Curve graph of the estimation angle of elbow motion: (a) estimated angle before and after smoothing (after TS-GAFS) and (b) estimated angle before and after TS-GAFS.

additional tests are given. Table X records the comparison results of different methods. As can be seen from Table X, the average of regression value R in this work is larger than the R of the initial data, and also larger than the R corresponding to the methods proposed by Xiao et al. [24] and Yang et al. [13]. However, there are still many problems that need to be solved. For example, adaptive window length needs to be applied when elbow joint motion changes rapidly. If a fixed window length is still used at this time, then features are calculated with the fixed window length, which will eventually lead to a poor angle prediction effect. In future work, the research on adaptive window length will be further developed. In addition,

TABLE IX
ESTIMATION PERFORMANCE UNDER THE LEAVE ONE-SUBJECT-OUT TEST

	Additional Test						Average
	Subject A	Subject B	Subject C	Subject D	Subject E	Subject F	
R	0.9607	0.9345	0.9522	0.9487	0.9228	0.9478	0.9445

TABLE X
COMPARISON OF PREDICTION PERFORMANCE WITH OTHER METHODS

	Channel Number	Features	R
Initial data	8	23	0.8971
Yang [13]	2	9	0.9080
Xiao [24]	2	5	0.9228
This paper	3	5	0.9445

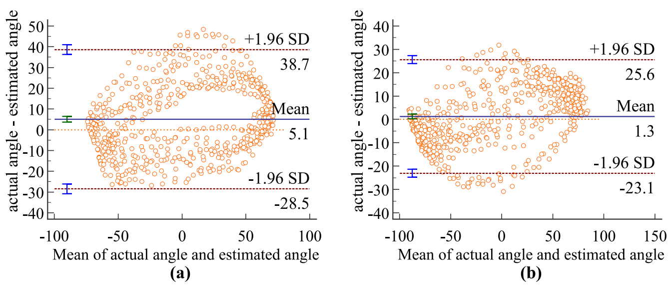

Fig. 6. B&A plots of the estimated angles and the target angles: (a) before TS-GAFS and (b) after TS-GAFS.

it is still a difficult problem to select feature sequences intelligently from sEMG signals, or even extract new feature sequences which are invariable among different users, which also needs further study. And the number of features involved in the first and second stages of the TS-GAFS method is also subject to further study to determine the optimal number of features. Achieving the subject-independent estimation of joint motion angle is our ultimate target, and an offline process has been implemented successfully. Therefore, our plans also include using the method proposed in this article for online angle estimation, and further applying it to the field of HRIs, such as combining the method with the control of portable upper limb exoskeleton rehabilitation devices using sEMG as the control signal.

V. CONCLUSION

In this article, a TS-GAFS method for subject-independent angle estimation based on the consideration of intersubject variability is proposed. In this method, the combination of GA and information theory is used to select the most common features among different subjects. The selected feature subset serves as the input of BPNN to achieve a better subject-independent estimation of elbow angles. The experiment shows that the proposed TS-GAFS can improve the overall accuracy of subject-independent angle estimation. In the future, the method proposed in this article will be further combined with real-time control of the exoskeleton for upper extremity rehabilitation.

APPENDIX

The full name of the TD features adopted in this article is as follows.

F1: Integrated absolute value (IAV).
F2: Mean absolute value (MAV).
F3: Root mean square (rms).
F4: Slope sign change (SSC).
F5: Zero-crossing (ZC).
F6: Auto regression model coefficients (ARC).
F7: Kurtosis (KURT).
F8: Exponent of logarithm (LogD).
F9: Margin factor (MarginFac).
F10: Maximum (MAX).
F11: Mean (MEAN).
F12: Minimum (MIN).
F13: Nonzero median (NZM).
F14: Peak factor (PeakFac).
F15: Peak-to-peak value (PK).
F16: Pulse factor (PulsFac).
F17: Skewness (SKEW).
F18: Simple square integral (SSI).
F19: Standard deviation (STD).
F20: Variance (VAR).
F21: Willison amplitude (WA).
F22: Waveform factor (WavFac).
F23: Waveform length (WL).

ACKNOWLEDGMENT

The authors would like to acknowledge all the subjects for participating in this study.

REFERENCES

[1] S. S. Virani et al., "Heart disease and stroke statistics—2020 update: A report from the American heart association," *Circulation*, vol. 141, no. 9, pp. 139–596, Mar. 2020, doi: 10.1161/CIR.0000000000000757.

[2] C. Wang, L. Peng, Z. Hou, J. Li, T. Zhang, and J. Zhao, "Quantitative assessment of upper-limb motor function for post-stroke rehabilitation based on motor synergy analysis and multi-modality fusion," *IEEE Trans. Neural Syst. Rehabil. Eng.*, vol. 28, no. 4, pp. 943–952, Apr. 2020, doi: 10.1109/TNSRE.2020.2978273.

[3] A. Keci, K. Tani, and J. Xhema, "Role of rehabilitation in neural plasticity," *Open Access Macedonian J. Med. Sci.*, vol. 7, no. 9, pp. 1540–1547, May 2019, doi: 10.3889/oamjms.2019.295.

[4] J. Chen, Y. Huang, X. Guo, S. Zhou, and L. Jia, "Parameter identification and adaptive compliant control of rehabilitation exoskeleton based on multiple sensors," *Measurement*, vol. 159, Jul. 2020, Art. no. 107765, doi: 10.1016/j.measurement.2020.107765.

[5] P. Arpaia, L. Duraccio, N. Moccaldi, and S. Rossi, "Wearable brain-computer interface instrumentation for robot-based rehabilitation by augmented reality," *IEEE Trans. Instrum. Meas.*, vol. 69, no. 9, pp. 6362–6371, Sep. 2020, doi: 10.1109/TIM.2020.2970846.

[6] Y. Liu, S. Guo, Z. Yang, H. Hirata, and T. Tamiya, "A home-based bilateral rehabilitation system with sEMG-based real-time variable stiffness," *IEEE J. Biomed. Health Informat.*, vol. 25, no. 5, pp. 1529–1541, May 2021, doi: 10.1109/JBHI.2020.3027303.

[7] Y. Liu, S. Guo, H. Hirata, H. Ishihara, and T. Tamiya, "Development of a powered variable-stiffness exoskeleton device for elbow rehabilitation," *Biomed. Microdevices*, vol. 20, no. 3, pp. 1–13, Aug. 2018, doi: 10.1007/s10544-018-0312-6.

[8] Z. Yang, S. Guo, Y. Liu, M. Kawanishi, and H. Hirata, "A task performance-based sEMG-driven variable stiffness control strategy for upper limb bilateral rehabilitation system," *IEEE/ASME Trans. Mechatronics*, vol. 28, no. 2, pp. 792–803, Apr. 2023, doi: 10.1109/TMECH.2022.3208610.

[9] D. Farina et al., "The extraction of neural information from the surface EMG for the control of upper-limb prostheses: Emerging avenues and challenges," *IEEE Trans. Neural Syst. Rehabil. Eng.*, vol. 22, no. 4, pp. 797–809, Jul. 2014, doi: 10.1109/TNSRE.2014.2305111.

[10] F. Wang, J. Lu, Z. Fan, C. Ren, and X. Geng, "Continuous motion estimation of lower limbs based on deep belief networks and random forest," *Rev. Sci. Instrum.*, vol. 93, no. 4, Apr. 2022, Art. no. 044106, doi: 10.1063/5.0057478.

[11] T. Bao, S. A. R. Zaidi, S. Xie, P. Yang, and Z. Zhang, "Inter-subject domain adaptation for CNN-based wrist kinematics estimation using sEMG," *IEEE Trans. Neural Syst. Rehabil. Eng.*, vol. 29, pp. 1068–1078, Jun. 2021, doi: 10.1109/TNSRE.2021.3086401.

[12] H. Li, S. Guo, D. Bu, and H. Wang, "Inter-subject variability evaluation of continuous elbow angle from sEMG using BPNN," in *Proc. IEEE Int. Conf. Mechatronics Automat. (ICMA)*, Guangxi, China, Aug. 2022, pp. 388–393, doi: 10.1109/ICMA54519.2022.9856005.

[13] Z. Yang, S. Guo, Y. Liu, H. Hirata, and T. Tamiya, "An intention-based online bilateral training system for upper limb motor rehabilitation," *Microsyst. Technol.*, vol. 27, no. 1, pp. 211–222, Jan. 2021, doi: 10.1007/s00542-020-04939-x.

[14] T. R. D. Saputri, A. M. Khan, and S. W. Lee, "User-independent activity recognition via three-stage GA-based feature selection," *Int. J. Distrib. Sens. Netw.*, vol. 10, no. 3, 2014, Art. no. 706287, doi: 10.1155/2014/706287.

[15] A. Xiong, X. Zhao, J. Han, G. Liu, and Q. Ding, "An user-independent gesture recognition method based on sEMG decomposition," in *Proc. IEEE/RSJ Int. Conf. Intell. Robots Syst. (IROS)*, Hamburg, Germany, Sep. 2015, pp. 4185–4190, doi: 10.1109/IROS.2015.7353969.

[16] (2013). *Thalmic Labs*. Accessed: Nov. 1, 2017. [Online]. Available: https://www.myo.com/

[17] C. Tepe and M. C. Demir, "The effects of the number of channels and gyroscopic data on the classification performance in EMG data acquired by Myo armband," *J. Comput. Sci.*, vol. 51, Apr. 2021, Art. no. 101348, doi: 10.1016/j.jocs.2021.101348.

[18] K. Li, J. Zhang, L. Wang, M. Zhang, J. Li, and S. Bao, "A review of the key technologies for sEMG-based human–robot interaction systems," *Biomed. Signal Process. Control*, vol. 62, Sep. 2020, Art. no. 102074, doi: 10.1016/j.bspc.2020.102074.

[19] J. Kim, B. Koo, Y. Nam, and Y. Kim, "SEMG-based hand posture recognition considering electrode shift, feature vectors, and posture groups," *Sensors*, vol. 21, no. 22, p. 7681, Nov. 2021, doi: 10.3390/s21227681.

[20] J. J. A. M. Junior, M. Freitas, H. Siqueira, A. E. Lazzaretti, S. Stevan, and S. F. Pichorim, "Comparative analysis among feature selection of sEMG signal for hand gesture classification by armband," *IEEE Latin Amer. Trans.*, vol. 18, no. 6, pp. 1135–1143, Jun. 2020, doi: 10.1109/TLA.2020.9099752.

[21] J. J. A. M. Junior, M. L. B. Freitas, H. V. Siqueira, A. E. Lazzaretti, S. F. Pichorim, and S. L. Stevan, "Feature selection and dimensionality reduction: An extensive comparison in hand gesture classification by sEMG in eight channels armband approach," *Biomed. Signal Process. Control*, vol. 59, May 2020, Art. no. 101920, doi: 10.1016/j.bspc.2020.101920.

[22] T. Naghibi, S. Hoffmann, and B. Pfister, "A semidefinite programming based search strategy for feature selection with mutual information measure," *IEEE Trans. Pattern Anal. Mach. Intell.*, vol. 37, no. 8, pp. 1529–1541, Aug. 2015, doi: 10.1109/TPAMI.2014.2372791.

[23] W. S. You, J. Casebier, J. Mandich, and R. Balasubramanian, "Genetic algorithm-based optimization for the geometric design of a novel orthopedic implant," *IEEE Trans. Biomed. Eng.*, vol. 68, no. 12, pp. 3620–3627, Dec. 2021, doi: 10.1109/TBME.2021.3080226.

[24] F. Xiao, Y. Wang, Y. Gao, Y. Zhu, and J. Zhao, "Continuous estimation of joint angle from electromyography using multiple time-delayed features and random forests," *Biomed. Signal Process. Control*, vol. 39, pp. 303–311, Jan. 2018, doi: 10.1016/j.bspc.2017.08.015.

He Li (Graduate Student Member, IEEE) received the M.S. degree from the School of Precision Instrument and Opto-Electronics Engineering, Tianjin University, Tianjin, China, in 2021. She is currently pursuing the Ph.D. degree with the Beijing Institute of Technology, Beijing, China.

She has authored five refereed journal articles and one conference paper. She researches on exoskeleton rehabilitation robots, surface electromyography (sEMG) signal processing, and telerehabilitation system.

Shuxiang Guo (Fellow, IEEE) received the Ph.D. degree in mechano-informatics and systems from Nagoya University, Nagoya, Japan, in 1995.

He is currently a Chair Professor with the Department of Electronic and Electrical Engineering, Southern University of Science and Technology, Shenzhen, Guangdong, China. He is also a Chair Professor with the Key Laboratory of Convergence System and Healthcare Technology Medical Engineering, The Ministry of Industry and Information Technology, Beijing Institute of Technology, Beijing, China. His research interests include medical robot systems, microcatheter systems, and biomimetic underwater robots.

Dr. Guo has a fellowship of The Engineering Academy of Japan.

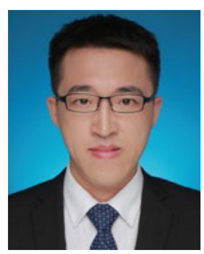

Dongdong Bu (Graduate Student Member, IEEE) received the M.S. degree in electronics and communication engineering from the Beijing Institute of Technology, Beijing, China, in 2017, where he is currently pursuing the Ph.D. degree.

He has authored four refereed journal articles and conference papers. He researches on exoskeleton rehabilitation robotic systems for biomedical applications.

Hanze Wang (Student Member, IEEE) received the B.S. degree from the School of Biomedical Engineering, Beijing Institute of Technology, Beijing, China, in 2021, where he is currently pursuing the M.S. degree.

He has authored one conference paper. He researches on exoskeleton rehabilitation robotic systems for biomedical applications.